Study of Monodispersed Polystyrene Colloidal Particles Containing Fluorine

Changsheng Liu, Jun Li

School of Material Science and Engineering, Wuhan Institute of Technology, Wuhan 430074, People's Republic of China

Received 2 February 2007; accepted 23 August 2007
DOI 10.1002/app.27270
Published online 23 April 2008 in Wiley InterScience (www.interscience.wiley.com).

ABSTRACT: Monodispersed polystyrene colloidal particles containing fluorine were synthesized by two-stage semicontinuous emulsion polymerization in the presence of trifluoroethyl methacrylate (F_3MA) as a functional comonomer. And then the colloidal crystal films were fabricated quickly from aqueous colloidal solutions by the vertical deposition method at certain temperature and humidity. The chemical components and thermal property of colloidal particles were determined by Fourier-transform infrared spectrometry and differential scanning calorimetry, respectively. The size and morphology of the particles were characterized by scanning electron microscopy (SEM). The surface element distribution of colloidal crystal films was measured by X-ray photoelectron spectroscopy (XPS). The optical property and water contact angles of the colloidal crystal films were investigated. When the concentration of F_3MA relative to the total content of monomers was 2.5%, the size and the coefficient of variation (C_v) of colloidal particles were 211 nm and 4.2%, respectively. The colloidal crystal film exhibited high water-contact angles (121.3°). The surface analysis by using XPS revealed that the fluorinated components preferentially enriched at the colloidal crystal film surface. © 2008 Wiley Periodicals, Inc. J Appl Polym Sci 109: 1604–1610, 2008

Key words: monodispersed particles; polystyrene; trifluoroethyl methacrylate; colloidal crystal

INTRODUCTION

Monodispersed colloidal particles have received much attention because such particles with optimized characteristics can be a good candidate in information technology, electric and electronic application, and biotechnology.[1–4] The ability to assemble these colloidal particles into crystalline arrays allows one to obtain interesting and useful functionalities not only from the application of constituent materials but also from the fundamental physics of systems with the long-range, mesoscopic order that characterizes periodic structures.[5] For example, two-dimensional hexagonal lattices of colloidal spheres have been successfully demonstrated as ordered arrays of optical microlenses in image processing[6]; as physical masks for evaporation or reactive ion etching to fabricate regular arrays of micro- or nanostructures; and as patterned arrays of relief structures to cast elastomeric stamps for use in soft lithographic techniques.[7] On the other hand, three-dimensional opaline lattices of colloidal spheres have recently been exploited as removable templates to generate highly ordered, macroporous materials[8]; as diffractive elements to fabricate sensors,[9] filters,[10] photonic crystals,[11] or other types of optical and electrooptical devices[12]; and as a directly observable (in three-dimensional real space) model system to study a wide variety of fundamental phenomena such as crystallization, phase transition, melting, and fracture mechanics.[13] All these applications strongly depend on the availability of colloidal particles with tightly controlled sizes, high monodispersity ($C_v < 5\%$), and functional groups. The polystyrene (PS) colloids are the preference for the applications because the PS colloidal spheres with excellent monodispersity can be easily produced by the classical emulsion polymerization method.[14]

Production of the monodispersed colloidal particles with special functional groups has been studied by several research groups. Wang and Pan[15] prepared uniform colloidal particles having carboxylic groups and investigated the distribution of carboxylic groups at the surface of colloidal particles. Park et al. prepared monodispersed PS particles having glycidyl-functional by seeded polymerization in aqueous medium.[16] Okubo and coworkers produced the monodispersed composite polymer particles

Correspondence to: C. Liu (liushen0880@sina.com).
Contract grant sponsor: National Science Foundation of China; contract grant number: 50343018.
Contract grant sponsor: National New and High Technology 863 Project; contract grant number: 2003AA302330.
Contract grant sponsor: Natural Science Foundation of Hubei Province; contract grant number: 2002AC006.

containing chloromethyl groups,[17] vinyl groups,[18] and epoxy groups[19] by seeded dispersion polymerization. In those composite particles produced, the functional groups preferentially distributed at the surface layers.

It is well known that the fluorinated segments in the fluorinated block or graft copolymers are easy to form a fluorine-covered surface, giving rise to a low surface energy and high surface activity.[20] For the same reason, if the fluorinated block or graft copolymer is incorporated with other polymer, the surface of such a polymer blend will be enriched by the fluorinated segments to show the low surface energy, even though there is only low concentration of the fluorinated block or graft copolymer in the blend system.[21–23] Linemann et al. used emulsion polymerization to prepare fluorine-containing polymer latex particles.[24] They found that the addition of acetone and butyl acrylate could lead to coagulation-free dispersions. Ha et al. used a cationic emulsifier to prepare a core-shell latex with a fluorinated polymethacrylate shell.[25]

In this research, monodispersed PS colloidal particles containing fluorine were synthesized by two-stage semicontinuous emulsion polymerization in the presence of trifluoroethyl methacrylate (F_3MA) as a functional comonomer. And then the colloidal crystal films were fabricated quickly from aqueous colloidal solutions by the vertical deposition method at certain temperature and humidity. The monodispersed PS colloidal particles containing fluorine were investigated by Fourier transfer infrared (FTIR), UV–vis, DSC, scanning electron microscopy (SEM), X-ray photoelectron spectroscopy (XPS), and contact angle goniometer.

EXPERIMENTAL

Materials

F_3MA was obtained from Aldrich (Milwaukee, WI) and used without further purification. Its purity was above 97%. Styrene (St) and methyl methacrylate (MMA) were washed with 5 wt % sodium hydroxide solution to remove inhibitors. The initiator, potassium persulfate (KPS), was purified by recrystallization. Sodium dodecylbenzensulfonate (SDBS) as the emulsifier and sodium bicarbonate ($NaHCO_3$) as the buffer were obtained from Guoyao Chemical Reagents Company, Shanghai, China. The deionized water was obtained by ion exchange.

Preparation of the monodispersed colloidal particles

The latex was synthesized by two-stage semi-continuous emulsion polymerization. Typically, the reaction was carried out under nitrogen atmosphere in a 250-mL four-neck flask equipped with a stirrer, a condensation tube, and a Celsius thermometer. In the first-stage, St, MMA, SDBS, KPS, and deionized water were added to the flask and completely emulsified, with stirring at 40°C for about 30 min. Next, the mixture was gradually heated to 85°C for 3 h in a water bath. The first-stage reaction was maintained at 85°C for about 2 h, which promised a high first-stage conversion. In the second-stage, the diluent aqueous solution of KPS at a concentration of 0.05 g/mL was slowly dropped into the reactor at a low speed of 1 drop/min. At the same time, the monomers containing St and F_3MA were dropped slowly into the reactor for about 2 h at 85°C. And then $NaHCO_3$ was added to control the pH of the reaction system in the range 6–7. Finally, the reaction was left at 85°C for an additional 2 h. The detailed recipe of the prepared samples and their final conversions are listed in Table I.

Fabrication of the colloidal crystal films

First, the dilute latex with a volume fraction of 0.1% was moved into a glass container, and then a clean glass microscope slide was placed oriented perpendicular to the liquid surface of the latex so that the glass was partially submerged. With the slow evaporation of water and the gradual increase of latex concentration, a crystalline deposit formed where the meniscus meets the slide surface by self-assembly. An optimized temperature and humidity for the fabrication process was observed at 65°C and 70%. Under these conditions, the growth speed of the film was 2–3 mm/h. After 12 h, the slide was picked up for further examination.[26]

Characterization

FTIR spectra of the latex particles were recoded with Nicolet Magna-FTIR750 spectrometer (Thermo Nicolet, Waltham, UK) in the range from 4000 to 400 cm^{-1}. The glass-transition temperatures (T_g) of polymers were measured with a CDR-4P differential scanning calorimeter (DSC) under nitrogen atmosphere at the heating rate of 10°C/min. All samples for analysis were purified three times through filtration and washed with ethanol to remove coagulate and soluble impurities. And then the samples were dried for several days under vacuum at 40°C.

The morphology of colloidal particles was observed by SEM (JEOL, JSM-5510LV, Japan). The number-average diameter (D_n) and the coefficient of variation (C_v) of particle diameter were defined using the following equations by counting at least 100 individual particles from SEM microphotographs.

TABLE I
The Recipe, Conversion, and Particle Characteristics of the Samples

	Sample 1	Sample 2	Sample 3	Sample 4
First stage (batch)				
St (g)	5.0	5.0	5.0	5.0
MMA (g)	0.50	0.50	0.51	0.50
SDBS (g)	0.1021	0.1017	0.1031	0.1011
KPS (g)	0.1523	0.1541	0.1532	0.1527
Water (g)	110.0	110.3	110.2	110.2
Conversion (%)	91.2	93.4	93.1	91.5
Second stage (semicontinuous)				
St (g)	15.0	14.5	14.0	13.0
F_3MA (g)	0	0.51	1.03	2.01
KPS (g)	0.3022	0.3096	0.3101	0.3074
Water (g)	6.12	6.08	6.03	6.10
$NaHCO_3$ (g)	0.1521	0.1517	0.1524	0.1511
Conversion (%)	94.8	92.6	88.9	82.7
Diameter[a] (nm)	232	219	198	143
Diameter[b] (nm)	227	212	193	\
C_V (%)	2.5	4.2	12.4	25.9

[a] Number-average diameter observed from SEM pictures.
[b] Average diameter calculated by Bragg equation.

$$D_n = \left(\sum n_i d_i / n_i\right) \quad (1)$$

$$C_V(\%) = \frac{\left(\sum (d_i - (\sum n_i d_i / \sum n_i))^2 \Big/ \sum n_i\right)^{1/2}}{(\sum n_i d_i / \sum n_i)} \quad (2)$$

where n_i is the number of particles having diameter d_i. The particle diameter (d_i) was estimated through SEM images and was defined as the equivalent diameter of equal-area circle.

The optical diffraction spectra of the colloidal crystal films were recorded using a UV-2550 spectrometer (Shimadzu, Japan). XPS data were collected in both survey and high-resolution mode on a KRATOS XSAM-800 with an Mg Kα source, operating at 300 W. Data were recorded at a 45° take-off angle, resulting in analysis depths of about 3 nm.

The solids content and conversion were measured by gravimetric analysis. A certain quantity of emulsion was cast onto a petri dish and dried to a constant weight in a dry oven at 75–85°C. The solids content and final conversion were calculated by the following formulas, respectively,

$$\text{Solid content } (\%) = \frac{W_2 - W_0}{W_1 - W_0} \times 100 \quad (3)$$

where W_0 is the weight of the petri dish, and W_1 and W_2 are the weights of emulsion before and after drying to constant weight, respectively.

$$\text{Conversion } (\%) = \frac{(\text{Solid content } (\%) \times W_3) - W_4}{W_5} \times 100 \quad (4)$$

where W_3 is the total weight of all the materials put in the flask in each polymerization, W_4 is the weight of materials that cannot volatilize when incinerating at 500°C for 5 h, and W_5 is the weight of total monomers.

Contact angles were measured by the sessile drop method at 25°C using a JGW-360B contact angle goniometer (Chengde Testing Machine, China). Typically, three drops of water were placed on the surface of the colloidal crystal films and three readings of contact angles were taken for each drop. The average of nine readings was used as the final contact angle of each sample.

RESULTS AND DISCUSSION

Chemical components of colloidal particles

Figure 1 shows the FTIR spectra of latex particles of (a) sample 1 and (b) sample 2. The characteristic absorption of the C=C bond at 1640 cm^{-1} disappeared, indicating that the monomers had polymerized. It is noteworthy that the unreacted monomers were a few and had evaporated during film formation, so their character peaks did not appear in the FTIR spectra. The characteristic peaks at 2849, 2923, 3000–3100, 760, and 700 cm^{-1} resulted from PS. The characteristic stretching peaks of C=O groups were strongly shown at 1748 cm^{-1} resulting from the fact that PMMA and PF_3MA all contain C=O groups. Compared with Figure 1(a), the FTIR spectrum of the fluorinated colloidal particles in Figure 1(b) shows many differences between 1100 and 1300 cm^{-1}, which are attributed to the peaks associated with motions of the fluoroethyl groups. The peak at

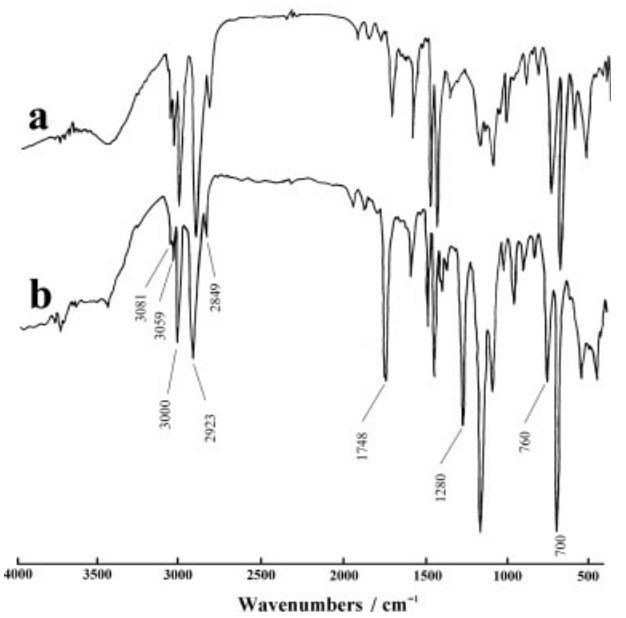

Figure 1 FTIR spectra of colloidal particles of (a) sample 1 and (b) sample 2.

1280 cm^{-1} in Figure 1(b) resulted from a combination of rocking and wagging vibrations of $—CF_3$ groups, which did not appear in Figure 1(a). This result proves that F_3MA participated in the polymerization.

DSC analysis

Figure 2 shows the DSC curves of the colloidal particles prepared. There was only one obvious temperature transform on each of the DSC curves, indicating that there was one T_g in all the latex polymers, e.g., samples 1–4 exhibited a T_g at 98.6, 98.1, 94.5, 89.6°C, respectively. Figure 2 also shows the effects of the concentrations of F_3MA relative to the total content of monomers on the polymer's T_g. The polymer's T_g became increasingly lower when the concentrations of F_3MA relative to the total content of monomers increased.

SEM analysis

Figure 3 represented the SEM pictures of colloidal particles synthesized with various F_3MA concentrations. It can be observed that the concentration of F_3MA relative to the content of monomers seems to have a significant influence on the particle size, the size distribution, and the morphology of the particles. The effects of the concentration of F_3MA on the polymerization characteristics are summarized in Table I. First, the conversion was decreased from 94.8% to 82.7% with an increase of concentration for F_3MA from 0 to 10 wt %. Second, the number-average diameter of colloidal particles was decreased from 232 to 143 nm. Third, the C_v value of colloidal particles was increased from 2.5 to 25.9%. The reason is that the solubility of F_3MA in water was lower than St; when the fluorinated monomers were added, some of them were not soluble and were not able to be incorporated into polymer; the redundant monomers formed the secondary particles. Because of the aforementioned reason, the ability to assemble colloidal particles into crystalline arrays is gradually deteriorated with an increase in the concentration of F_3MA.

UV–vis analysis

Figure 4 shows the transmission spectrum of colloidal crystal film obtained from samples 1 to 4. It can be observed that the strength of the diffraction peak decreased gradually with an increasing concentration of F_3MA. When the concentration of F_3MA was 10 wt %, the diffraction peak disappeared. The strength of diffraction peak reflected the order degree of colloidal crystal. The strength of diffraction peak decreased when the order degree of colloidal crystal was poor.[26] So the order degree of colloidal crystal decreased with the increase of F_3MA concentration. In addition, according to Figure 4, the wavelength of diffraction peak shifted from long wavelength to short wavelength with F_3MA concentration increasing. The wavelength of diffraction peak reflected the center-to-center distance of colloidal spheres or the diameter of the spheres. The wavelength of diffraction peak decreased when the diameter of colloidal spheres decreased.[27] The relationship between the positions of diffraction peaks (λ_{max}) and diameter of colloidal spheres (D) can be approximately identified using Bragg eq. (5) for first-order diffraction[28]:

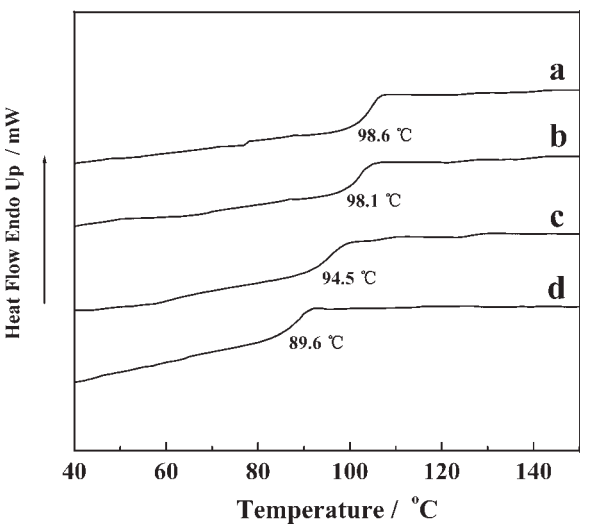

Figure 2 DSC curves of colloidal particles prepared. Concentrations of F_3MA relative to the total content of monomers: (a) 0 wt %, (b) 2.5 wt %, (c) 5 wt %, (d) 10 wt %.

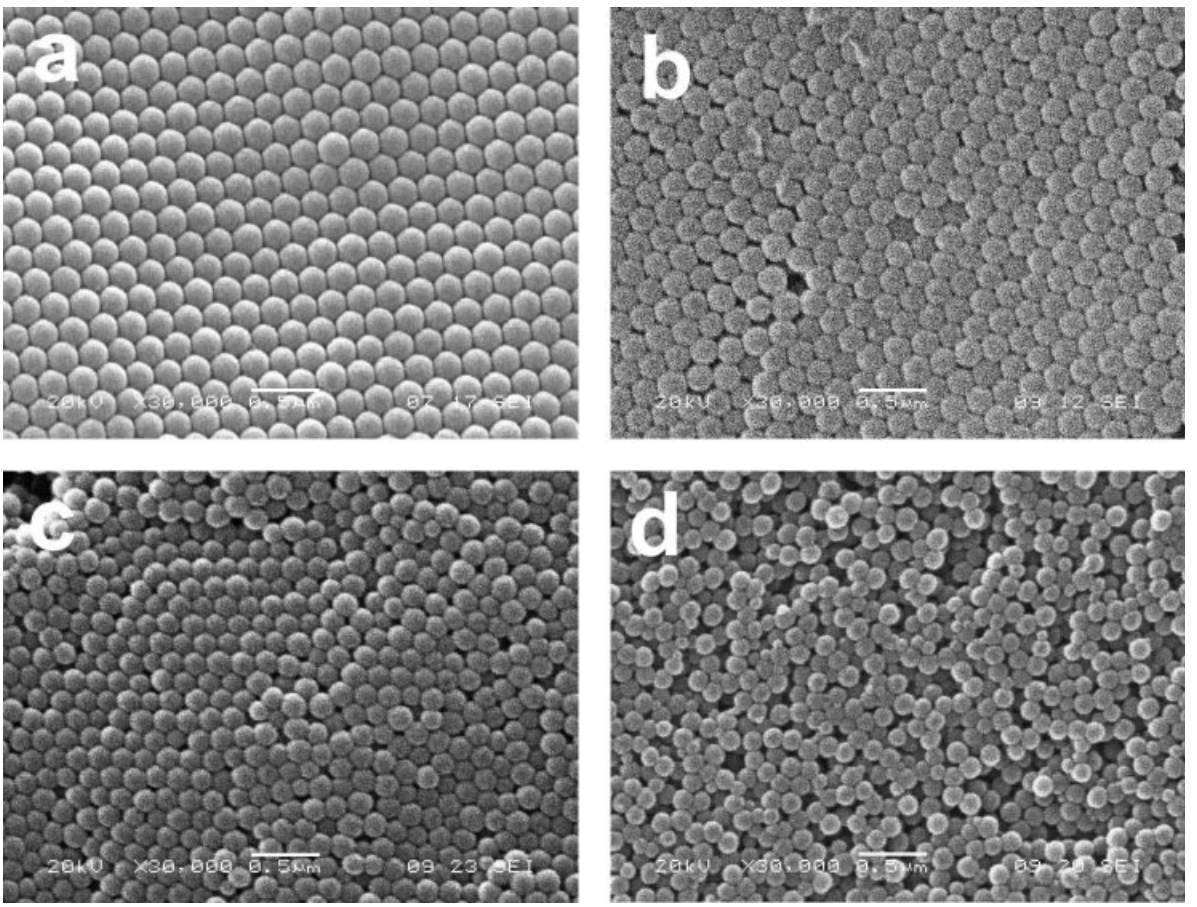

Figure 3 SEM pictures of the colloidal particles prepared. Concentrations of F_3MA relative to the total content of monomers: (a) 0 wt %, (b) 2.5 wt %, (c) 5 wt %, (d) 10 wt %.

$$\lambda_{max} = (8/3)^{1/2} D(n_{sphere}^2 V_{sphere} + n_{void}^2 V_{void} - \sin^2 \phi)^{1/2} \quad (5)$$

where D is the center-to-center distance of colloidal spheres or equivalent to the diameter of the spheres in this study. n_{sphere} and n_{void}, the refractive index of the spheres and voids, respectively, are 1.6 for spheres and 1 for air voids. V_{sphere} and V_{void}, the volume fractions of spheres and voids, are 0.74 and 0.26, respectively, in the fcc structure. Φ is the angle between incident light beam and the normal to the surface of the colloidal crystal film, sin Φ is 0 in this study. Apparently, the results agreed with the SEM images in Figure 3 by and large. The number-average diameter obtained by SEM and the average diameter calculated by Bragg equation are listed in Table I.

Surface properties of colloidal crystal films

XPS analysis

Figure 5 shows the surface composition of the colloidal crystal film obtained from sample 2, determined by an XPS analysis at a take-off angle of 45°. Three signals were presented in the survey spectra [Fig. 5(a)]: at 285, 532, 688 eV, due to electrons ejected from C1s, O1s, and F1s orbitals, respectively. The high-resolution signals, corresponding to the carbon

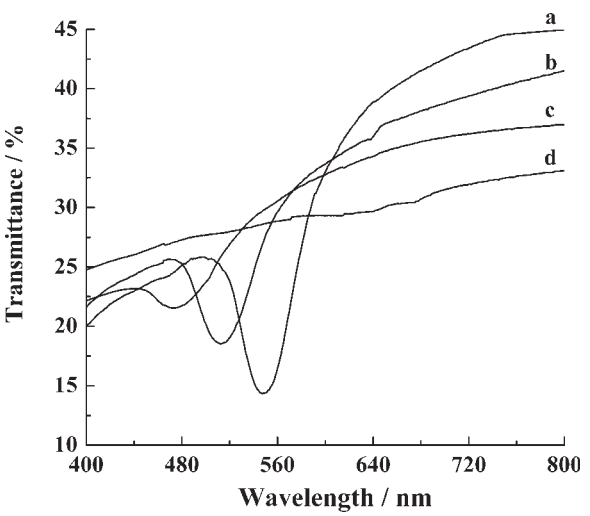

Figure 4 UV–vis spectra of the colloidal crystal films prepared. Concentrations of F_3MA relative to the total content of monomers: (a) 0 wt %, (b) 2.5 wt %, (c) 5 wt %, (d) 10 wt %.

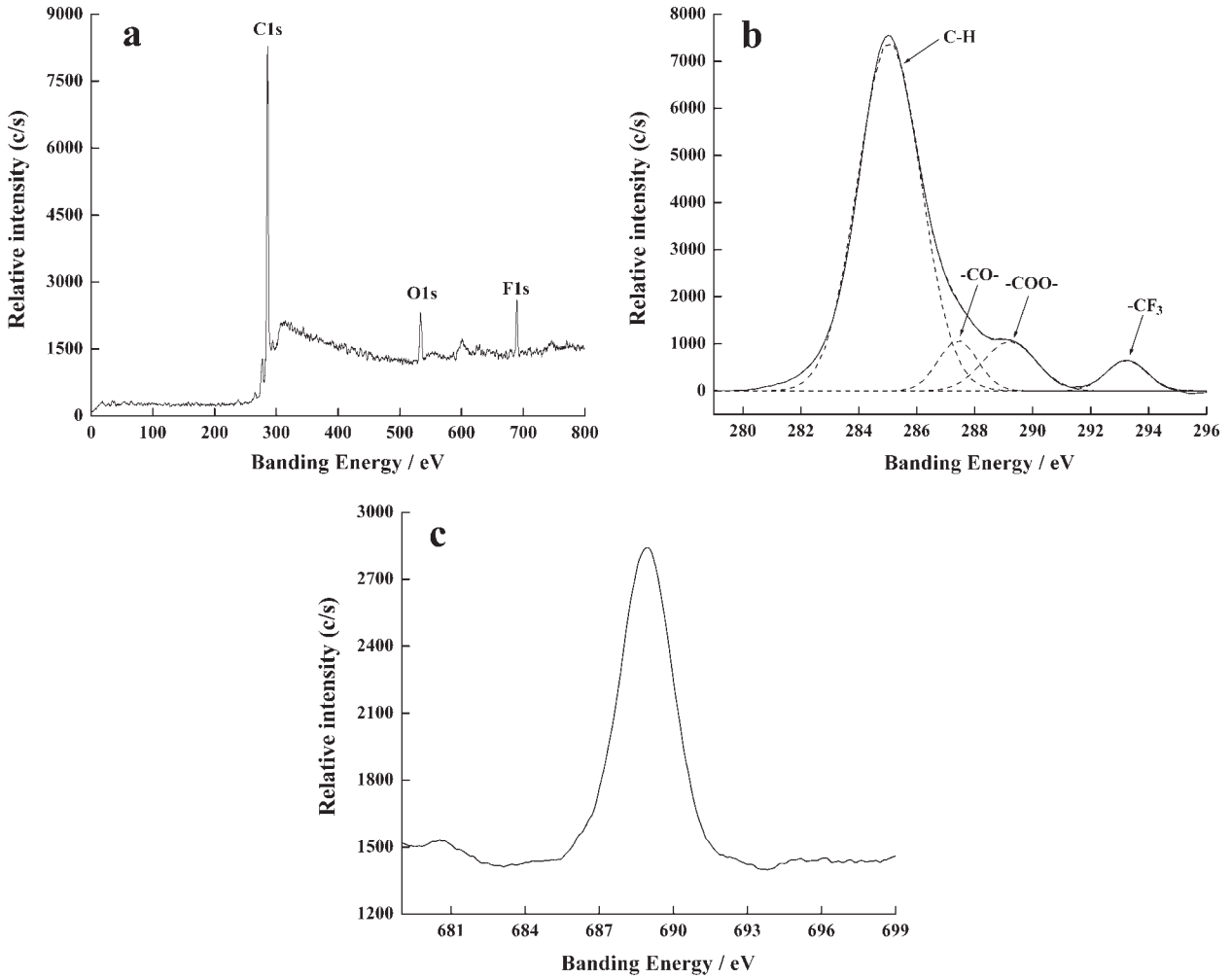

Figure 5 XPS spectra of the colloidal crystal film obtained from sample 2: (a) survey spectra; (b) C1s peaks; (c) F1s peaks.

atom and fluorine atom, are shown in Figure 5(b,c). It is worth noting that the C1s signal consisted of four components. Besides the one centered at 284.8 eV (corresponding to aliphatic and aromatic carbon atoms) and that at 287.2, 289.1 eV (corresponding to carbon in —CO— and —COO— groups, respectively), there is also a signal at 293.2 eV due to carbon atoms combined with the fluorine atoms (—CF_3). In addition, the intensity of the fluorine signal at 688.3 eV of colloidal crystal film was very strong [shown in the Fig. 5(c)], indicating the preferential concentration of fluorine at the surface and the F_3MA participated in the polymerization as discussed previously.

Contact angle analysis

The water contact angles of the colloidal crystal films are listed in Table II. The water contact angles of the colloidal crystal films with fluorine were all above 110°, whereas the water contact angle of the colloidal crystal film without fluorine was 102.4°C, indicating that the wetting-resistant property of the films were enhanced. The maximum contact angle (121.3°) occurred when the concentration of F_3MA relative to total content of monomers was 2.5 wt %. But the water contact angles of the colloidal crystal films with fluorine decreased with an increase in concentrations of F_3MA dramatically.

TABLE II
Water Contact Angle of the Colloidal Crystal Films Prepared with Different Concentrations of F_3MA

	Sample 1	Sample 2	Sample 3	Sample 4
Concentration of F_3MA (wt %)	0	2.5	5.0	10.0
Contact angle (°)	102.4	121.3	113.7	110.4

CONCLUSION

The monodispersed PS colloidal particles containing fluorine were synthesized by two-stage semicontinuous emulsion polymerization in the presence of F_3MA as a functional comonomer. And then the colloidal crystal films were fabricated quickly from aqueous colloidal solutions by the vertical deposition method. When the concentration of F_3MA relative to the total content of monomers was 2.5 wt %, the size and the coefficient of variation (C_v) of colloidal particles were 211 nm and 4.2%, respectively. The colloidal crystal film exhibited high water-contact angles (121.3°). The surface analysis by using XPS revealed that the fluorinated components preferentially enriched at the colloidal crystal film surface.

References

1. Fudouz, H.; Xia, Y. N. Adv Mater 2003, 15, 892.
2. Bhatt, K. H.; Grego, S.; Velev, O. D. Langmuir 2005, 21, 6603.
3. Ugelstad, J.; Stenstad, P.; Kilaas, L.; Prestvik, W. S.; Rian, A.; Nustad, K.; Herje, R.; Berge, A. Macromol Symp 1996, 101, 491.
4. Covolan, V. L.; Mei, L. H. I.; Rossi, C. L. Polym Adv Technol 1997, 8, 44.
5. Lin, K.-H.; Crocker, J. C.; Prasad, V.; Schofield, A. Phys Rev Lett 2000, 85, 1770.
6. Hayashi, S.; Kumamoto, Y.; Suzuki, T.; Hirai, T. J Colloid Interface Sci 1991, 144, 538.
7. Xia, Y. N.; Tien, J.; Qin, D.; Whitesides, G. M. Langmuir 1996, 12, 4033.
8. Velev, O. D.; Tessier, P. M.; Lenhoff, A. M.; Kaler, E. W. Nature 1999, 401, 548.
9. Lee, Y. J.; Pruzinsky, S. A.; Braun, P. V. Langmuir 2004, 20, 3096.
10. Mach, P.; Wiltzius, P.; Megens, M.; Weitz, D. A.; Lin, K. H.; Lubensky, T. C.; Yodh, A. G. Europhys Lett 2002, 58, 679.
11. Velev, O. D.; Jede, T. A.; Lobo, R. F.; Lenhoff, A. M. Nature 1997, 389, 447.
12. Kuncicky, D. M.; Prevo, B. G.; Velev, O. D. J Mater Chem 2006, 16, 1207.
13. Grier, D. G. MRS Bull 1998, 23, 21.
14. Okubo, M., Ed. Polymer Particles, Vol. 175; Springer-Verlag: Netherlands, 2005.
15. Wang, P. H.; Pan, C.-Y. Colloid Polym Sci 2001, 279, 98.
16. Park, J.-G.; Kim, J.-W.; Suh, K.-D. Colloid Polym Sci 2001, 279, 638.
17. Okubo, M.; Ikegami, K.; Yamamoto, Y. Colloid Polym Sci 1989, 267, 193.
18. Yamamoto, Y.; Okubo, M.; Iwasaki, Y. Colloid Polym Sci 1991, 269, 1126.
19. Okubo, M.; Okada, M.; Miya, T.; Takehoh, R. Colloid Polym Sci 2001, 279, 807.
20. Boker, A.; Reihs, K.; Wang, J. G.; Stadler, R.; Ober, C. K. Macromolecules 2000, 33, 1310.
21. Yang, S.; Wang, J.; Ognio K.; Valiyaveettil, S. Low-suface-energy fluoromethacrylate block copolymers with patternable elements. Chem Mater 2000, 12, 33.
22. Saidi, S.; Guittard, F.; Geribaldi, S. Polym Int 2002, 51, 1058.
23. Torstenssin, M.; Ranby, B.; Hult, A. Macromolecules 1990, 23, 126.
24. Linemann, R. F.; Malner, T. E.; Brandsch, R.; Bar, G.; Ritter, W.; Mülhaupt, R. Macromolecules 1999, 32, 1715.
25. Ha, J.-W.; Park, I. J.; Lee, S.-B.; Kim, D.-K. Macromolecules 2002, 35, 6811.
26. Wang, J.; Yuan, C.-W.; Huang, Z.-B.; Tang, F.-Q. Acta Phys Sin 2004, 53, 3054.
27. Allard, M.; Sargent, E.; Kumacheva, E.; Kalinina, O. Opt Quantum Electron 2002, 34, 27.
28. Gu, Z.-Z.; Fujishima, A.; Sato, O. Chem Mater 2002, 14, 760.